Experimental testing and modelling of a mechanical steering compensator

Jason Z. Jiang, Malcolm C. Smith and Neil E. Houghton

***Abstract*—This paper describes experimental results for a prototype mechanical steering compensator for motorcycles which was manufactured at Cambridge University Engineering Department (CUED). The compensator realises a mechanical network consisting of inerters, dampers and a spring. The paper extends the previous work of Papageorgiou et al and presents frequency response testing results as well as model fitting and parameter estimation.**

I. Introduction

This paper describes a second set of experiments carried out at Cambridge University Engineering Department (CUED) on a prototype mechanical steering compensator for motorcycles. The compensator realises a mechanical network consisting of inerters, dampers and a spring. The use of such a compensator for the control of motorcycle steering oscillation is described in [1], [2]. Relevant background on the inerter can be found in [6], [8], [9]. The first set of experiments on the device was reported in [7]. During the analysis of the results in [7], it was discovered that the friction in the device was approximately 10 times greater than anticipated. The source of the discrepancy was then discovered to be an inadequate clearance within the device which was then corrected. This report documents the frequency response testing results obtained with the modified device. Comparison of the two sets of data, and model fitting are described.

II. Steering Compensator Testing

A. The steering compensator and hydraulic test rig

A prototype steering compensator was manufactured in the Cambridge University Engineering Department workshops to investigate the more practical mechanical design issues following the work of [1], [2]. The prototype steering compensator device is shown in Fig. 1. It has a mass of 1.48 kg, maximum instantaneous torque rating of 60 Nm, length 187 mm and diameter 71 mm. The output side of the gear box is connected to a disc of small inertia and a flywheel is allowed to spin freely on the same shaft. The disc and the flywheel are both located inside the cylindrical casing shown in Fig. 1. Between them there is a small clearance occupied by oil which is responsible for transferring torque from the disc to the flywheel to create the effect of a linear damper. The flywheel accounts for the main inertance of the device while the disc gives rise to a small parasitic inertance. Oils of different viscosity can be used in order to vary the damping. There is also a spring effect associated with the device due to the elasticity of the gearbox. Although the device is rotational, the use of a lever arm in testing means that it can be modelled as a translational device in the subsequent analysis. The translational inertance, damper rate and spring rate are given by their rotational counterparts multiplied by the inverse of the lever arm squared 0.05^{-2} m^{-2}.

Jason Z. Jiang zj219@cam.ac.uk Malcolm C. Smith mcs@eng.cam.ac.uk and Neil E. Houghton neh27@cam.ac.uk are with the Department of Engineering, University of Cambridge, Cambridge CB2 1PZ, UK

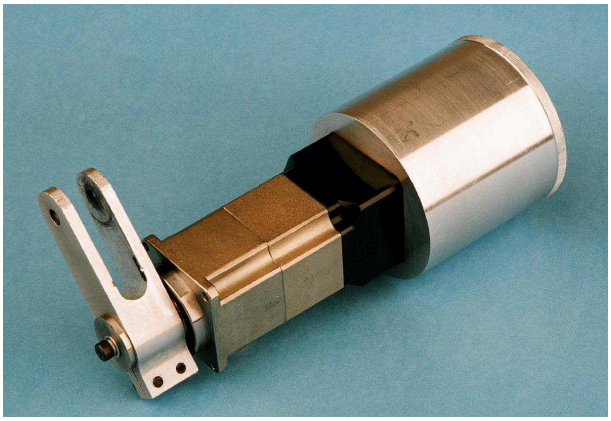

Fig. 1. The steering compensator device.

A Schenk hydraulic rig was used to test the steering compensator. The displacement of the hydraulic ram is controlled in closed-loop with a PID controller and the device to be tested can be placed between the hydraulic ram and a fixed point directly above it.

The identification procedure for the calculation of the admittance of the device involves 3 steps. Firstly, the steering compensator is excited by sinusoidal signals in an appropriate frequency range. The demand displacement, the actual ram displacement and the force through the device are recorded at each frequency. Secondly, using the correlation method [3, p.143] the gain and phase of the transfer function from the demanded displacement to the actual ram displacement ($\hat{x}/\hat{x}_{dem}$) and the force respectively ($\hat{F}/\hat{x}_{dem}$) are calculated (where $\hat{\cdot}$ denotes Laplace transform). Finally, the experimental estimate of the admittance function $\hat{F}/(s\hat{x})$ of the device is then deduced directly from this pair of gain and phase estimates. A more detailed description of the testing setup and identification procedure is given in [7], [6].

B. Experiment results and analysis

1) Testing results: The experimental admittance of the steering compensator was calculated for four different oils using 33 logarithmically spaced frequency points in the range

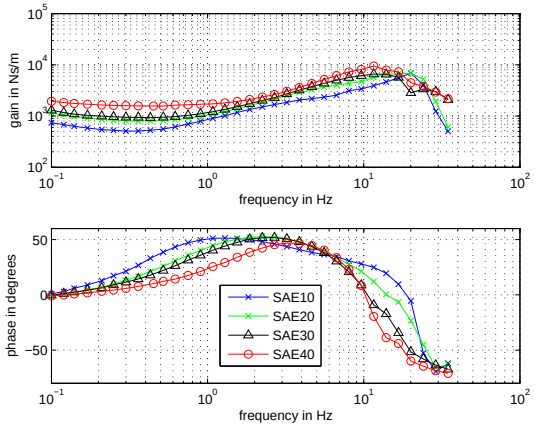

Fig. 2. Comparison of admittance functions for new experiments.

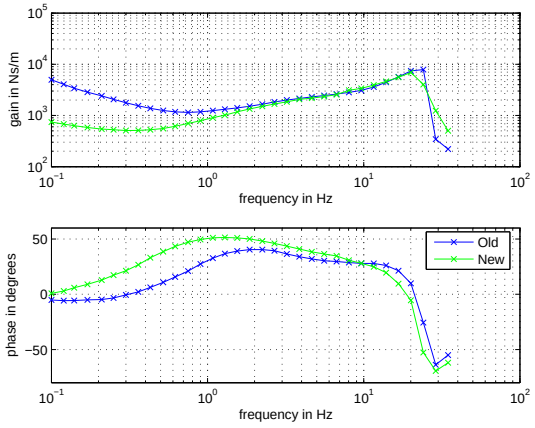

Fig. 3. Comparison of old and new admittance function for the SAE10 oil.

$[0.1, 35]$ Hz. The admittance for each oil is shown in Fig. 2. The SAE40 oil has the largest viscosity while the SAE10 oil has the smallest viscosity.

In the previous experiments the amplitude was chosen in advance based on the expected admittance and to satisfy two requirements: i) actual displacement $\leq$ 13 mm; ii) force through device $\leq$ 550 N. Even though the exact admittance was not known in advance, this was sufficient to provide an appropriate excitation level, except at high frequencies. At such frequencies, due to the presence of backlash and the fact that the actual displacement is very small, the force through the device is reduced. In the new experiments it was decided to boost the demand displacement manually for frequencies above 10 Hz. This was carried out for oils SAE30 and SAE40 (except at the frequency 20.05 Hz for the SAE30 oil due to an oversight).

2) Comparison with old testing results: The modified device was expected to have approximately 10 percent of the friction of the previous device. The effect of friction is to boost the gain and lower the phase at low frequencies. Comparing the old and new experimental data for all 4 oils (Fig. 3-6), we can see both differences.

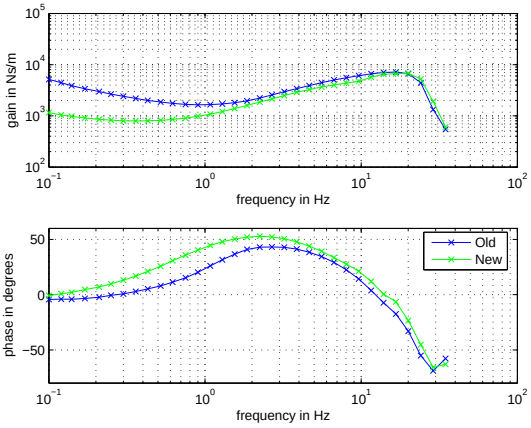

Fig. 4. Comparison of old and new admittance function for the SAE20 oil.

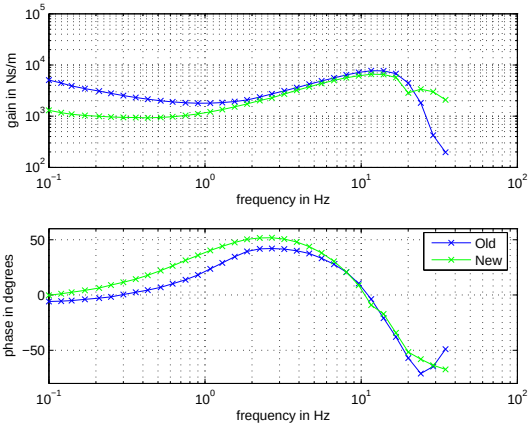

Fig. 5. Comparison of old and new admittance function for the SAE30 oil.

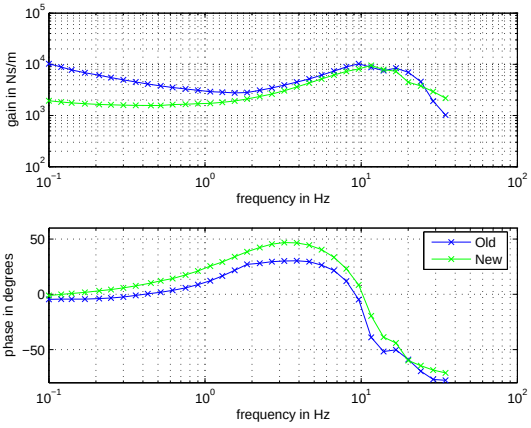

Fig. 6. Comparison of old and new admittance function for the SAE40 oil.

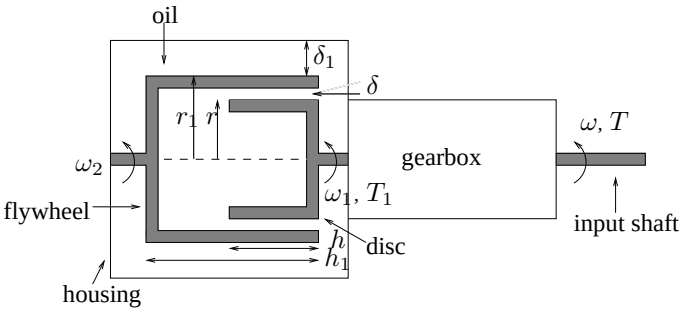

Fig. 7. Schematic of the physical model of the steering compensator.

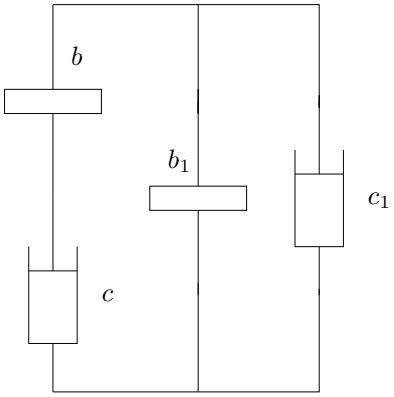

Fig. 8. The first linear model of the steering compensator.

III. Steering Compensator Modelling

A. Ideal linear model

1) Derivation of linear model and physical parameter estimates: A schematic of a physical model of the steering compensator is shown in Fig. 7. The model consists of a rotational gearbox (n : 1), a disk of relatively small inertia J_1 connected rigidly to the output shaft, and a second inertia J_2 (the flywheel) which may rotate independently of J_1. The assembly is contained in a housing filled with oil intended to provide a linear damping with coefficient γ between the disc and the flywheel by means of a small clearance δ between the two cylindrical surfaces. Additionally, there is a smaller damping with coefficient γ_1, acting directly on the flywheel due to the clearance δ_1 between the flywheel and the housing. From Massey [4, p.175], the damping coefficient can be estimated from the formula

$$\gamma = \frac{4\pi h \left(r+\delta\right)^2 r^2 \mu}{\delta\left(2r+\delta\right)} \tag{1}$$

where μ is the viscosity of the oil. There is a similar formula for γ_1 in which δ, r and h are replaced by δ_1, r_1 and h_1. We can write down the modelling equations of the compensator as follows:

$$\begin{aligned} T_1 &= n^{-1}T, \\ \omega_1 &= n\omega, \\ T_1 &= J_1\dot{\omega_1} + \gamma\left(\omega_1 - \omega_2\right), \\ J_2\dot{\omega_2} &= \gamma\left(\omega_1 - \omega_2\right) - \gamma_1\omega_2. \end{aligned}$$

We can verify that the admittance function of the compensator is given by

$$\begin{aligned} \frac{\hat{T}}{\hat{\omega}} =& n^2\left(sJ_1 + \gamma - \frac{\gamma^2}{sJ_2+\gamma+\gamma_1}\right) \\ =& n^2\Bigg(sJ_1 + \frac{\gamma\gamma_1}{\gamma+\gamma_1} + \left(\left(\frac{\gamma^2}{\gamma+\gamma_1}\right)^{-1}\right. \\ &\left. + \left(\frac{\gamma^2 J_2 s}{\left(\gamma+\gamma_1\right)^2}\right)^{-1}\right)^{-1}\Bigg). \end{aligned}$$

The network corresponding to this linear admittance function is shown in Fig. 8 in which

$$b = n^2\left(\frac{\gamma}{\gamma+\gamma_1}\right)^2 J_2, \quad b_1 = n^2 J_1$$
$$c = n^2\frac{\gamma^2}{\gamma+\gamma_1}, \quad c_1 = n^2\frac{\gamma\gamma_1}{\gamma+\gamma_1}.$$

The physical parameters of the compensator are shown in Table I, and the parameters ν (kinematic viscosity) and ρ (density) for the four oils at 20 °C are shown in Table II, where $\mu = \nu/\rho$. From these values we can estimate the physical parameters to be the values given in Table III.

2) Optimization method: The experimental admittance functions were initially compared to those of an ideal linear model shown in Fig. 8 together with a series spring associated

TABLE I
The physical parameters of the compensator.

Parameters	Values
r	27.5 mm
r_1	30 mm
δ	0.1 mm
δ_1	2 mm
h	13.8 mm
h_1	27.5 mm
J_1	2.16×10^{-5} kgm^2
J_2	9.84×10^{-5} kgm^2
n	50

TABLE II
The kinematic viscosity and density for SAE10-40 at 20 °C.

SAE@20 °C	ν, mm^2/s	ρ, kg/litre
10	115-130	0.875
20	200	0.885
30	350	0.89
40	900	0.9

TABLE III
The network parameters estimates.

SAE@20 °C	b, kg	b_1, kg	c, Ns/m	c_1, Ns/m
10	77	21.6	1966	254.31
20	77	21.6	3209.7	415.2
30	77	21.6	5617	726.6
40	77	21.6	14443.7	1868.4

TABLE IV
THE ESTIMATED PARAMETERS FOR ALL FOUR OILS (OBJECTIVE FUNCTION USING ALL FREQUENCIES).

Parameter	Linear equivalent value
k	443.740 kN/m
c,c_1 for SAE10	[1696.5,395] Ns/m
c,c_1 for SAE20	[2946.8,684.4] Ns/m
c,c_1 for SAE30	[3912.5,833.56] Ns/m
c,c_1 for SAE40	[5789.7,1500.9] Ns/m

with gearbox compliance. The value of the spring stiffness specified by the manufacturer is 1200 Nmrad^{-1} (rotational) which is equivalent 480 kNm^{-1} (translational). This model is illustrated in Fig. 9.

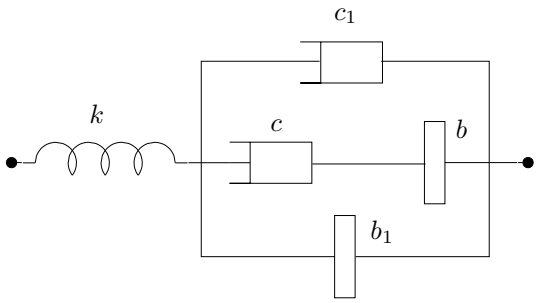

Fig. 9. The linear model of the steering compensator.

To estimate the linear model parameters the following criterion was considered:

$$J_{oil} = \sum_{i=1}^{n_f} \frac{|Y(p, jw_i) - E_{oil}(jw_i)|}{|E_{oil}(jw_i)|} \quad (2)$$

in which n_f is the number of frequency points, the decision variable is given by $p = [c, c_1, k, b_1, b]$ and $E_{oil}(jw_i)$ is the experimental admittance function corresponding to a specific oil (SAE10, SAE20 etc). The term $Y(p, jw_i)$ is the admittance function which is calculated from the admittance of the linear model using the frequency correlation method and the same excitation inputs as the ones used for the calculation of the experimental admittance functions. The optimization was solved using the Matlab function *fmincon*.

3) Optimization results for four oils: A combined optimization was carried out for all four oils together in which b and b_1 were fixed at the values $n^2 J_2 = 98.4$ kg and $n^2 J_1 = 21.6$ kg for all four cases. The objective function $J_{oil} = J_{SAE10} + J_{SAE20} + J_{SAE30} + J_{SAE40}$ was optimized over 9 parameters: a single variable k for all 4 oils, and c, c_1 for the four types of oil. The optimisation results are shown in Table IV.

B. Inclusion of a friction model and a backlash model in the steering compensator

To properly model the behaviour of the device at low frequencies, a friction model was needed. Bench measurements on the gear box indicated linear friction equivalents as follows: static friction $f_s = 2$ N and dynamic friction $f_d = 1.75$ N. The model of the steering compensator was further augmented

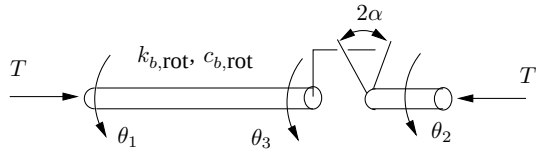

Fig. 10. Schematic of the backlash model.

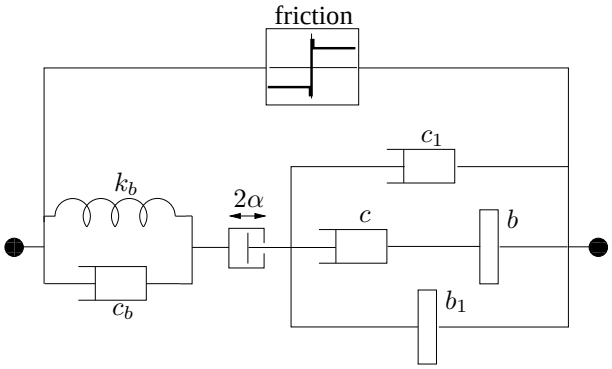

Fig. 11. The model of the steering compensator with friction and backlash.

by including a rotational backlash model in the gearbox to try to get a better fit at high frequencies. The backlash model was taken from [5] and consists of an inertia-free shaft with a backlash gap 2α rad, and a spring with elasticity $k_{b,\text{rot}}$ (Nm/rad) in parallel with a viscous damping $c_{b,\text{rot}}$ (Nm/rad) as shown in Fig. 10. The steering compensator model including the friction and the backlash is shown in Fig. 11. The same cost function and the same optimization procedure was used for the estimation of the model parameters. The decision variable is now given by $p = [k_b, b, b_1, \alpha]$ with c, c_1 held fixed for each of the 4 oils at the values given in Table V. For the optimisation, the actual displacement excitation given to the model is the same as the displacement used in the experiments.

The estimated backlash gap ($2\alpha = 11$ arc min) is somewhat larger than the maximum backlash specification of the gearbox (5 arc min). The extra backlash is attributed to play in the linkages, e.g. between the lever arm and driving rod. (The translational play for a backlash gap of $2\alpha = 0.0032$ rad is equal to 0.16 mm). The extra backlash due to the linkages etc. observed in these experiments is lower than that experienced in [7]. This is consistent with the fact that the pin between the lever arm and driving rod was replaced before the present experiments. The estimated spring stiffness k_b is a little lower than the gearbox compliance specified by the manufacturer (480 kN/m). From Figs. 12-15, we can see that the model fits the high frequency experimental data better than the model without backlash. Indeed, the same model gives a reasonable fit to the data with boosted amplitude as well as non-boosted amplitude. See especially the high frequency behaviour for the SAE10 and SAE20 oils and the anomalous point at 20.05 Hz for the SAE30 oil.

C. Comparison of experimental and theoretical time responses

In this section we present a brief comparison between the theoretical and the experimental time responses for the

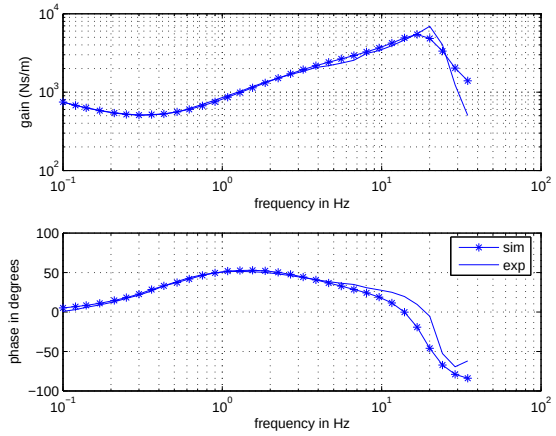

Fig. 12. The experimental and optimized admittance functions for the SAE10 oil with friction and backlash included.

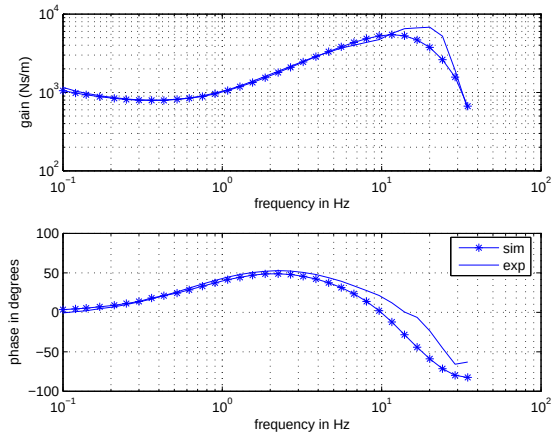

Fig. 13. The experimental and optimized admittance functions for the SAE20 oil with friction and backlash included.

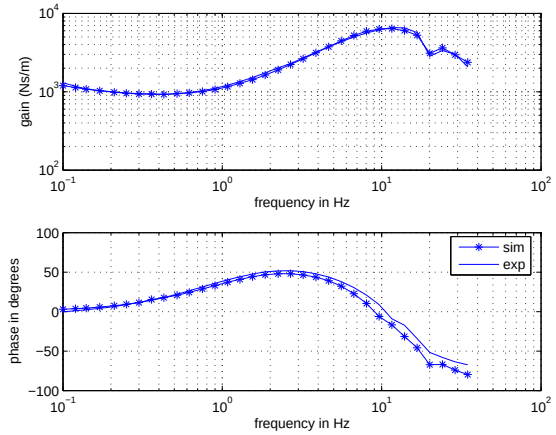

Fig. 14. The experimental and optimized admittance functions for the SAE30 oil with friction and backlash included.

TABLE V
THE ESTIMATED PARAMETERS FOR 4 OILS WITH BACKLASH INCLUDED

Parameter	Linear equivalent value
k_b	443.740 kN/m
b	78.72 kg
b_1	23.47 kg
α	0.0019 rad

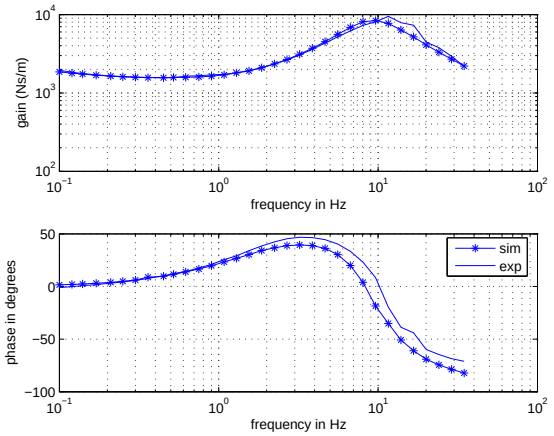

Fig. 15. The experimental and optimized admittance functions for the SAE40 oil with friction and backlash included.

SAE30 oil. Time responses at four frequency points namely, $f = 0.1,\ 3.22,\ 8.04,$ and 20.05 Hz have been compared in Figs. 16-19. The theoretical and experimental time responses agree fairly well for the four frequencies.

IV. CONCLUSIONS

A second set of experiments was performed to identify the frequency response of a prototype mechanical steering compensator. Model fitting was carried out on the new experimental data.

Two main differences were found with the previous set of model parameters. Firstly, the friction was about ten times

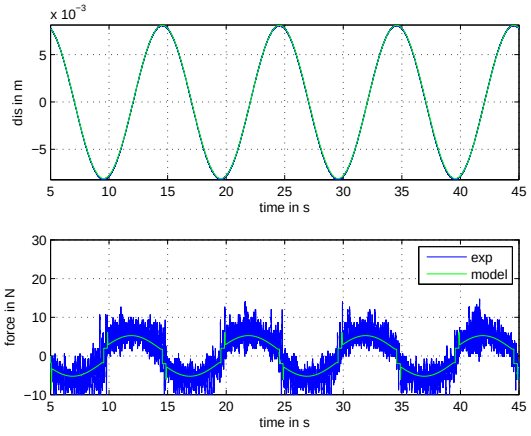

vol.

Fig. 16. Comparison of theoretical and experimental time responses at $f = 0.1$ Hz for the SAE10 oil.

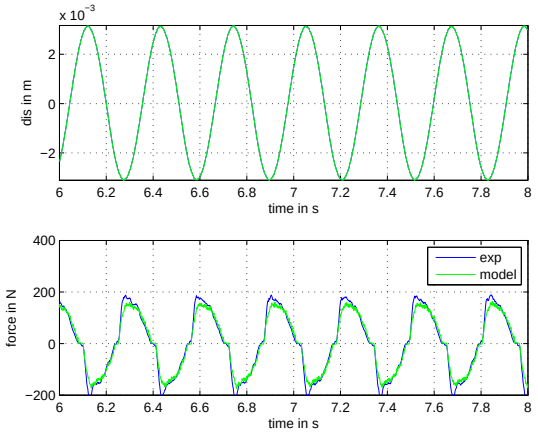

Fig. 17. Comparison of theoretical and experimental time responses at $f = 3.22$ Hz for the SAE20 oil.

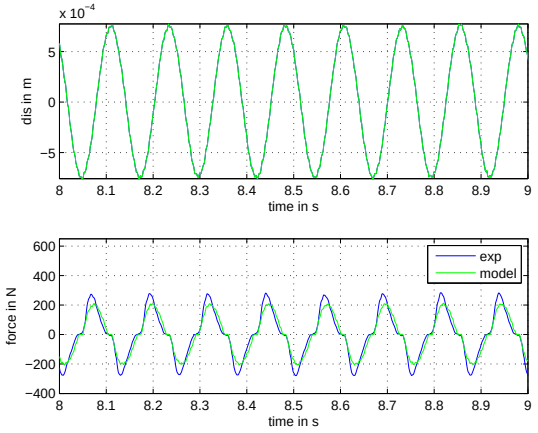

Fig. 18. Comparison of theoretical and experimental time responses at $f = 8.04$ Hz for the SAE30 oil.

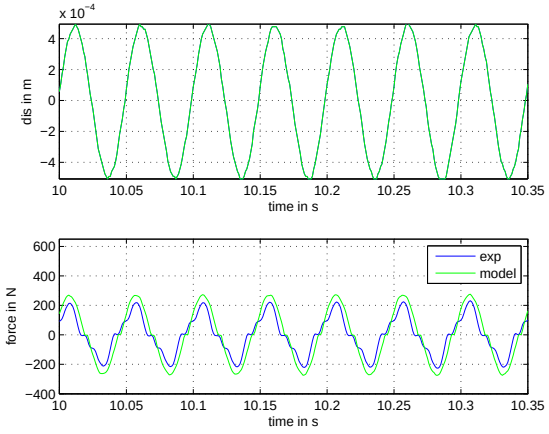

Fig. 19. Comparison of theoretical and experimental time responses at $f = 20.05$ Hz for the SAE40 oil.

lower, as expected. Secondly, the amount of backlash was observed to be lower, which is consistent with the attempt to reduce the backlash in the linkages.

All elements of the model have been explained physically and the parameter values obtained after optimisation are reasonably close to the physical parameter estimates. The new experiments made use of larger demand displacements at higher frequencies for two of the oils in order to better identify the high frequency dynamics. The backlash model was successful in explaining the data for both cases of boosted and non-boosted amplitudes. It can be seen from the comparisons of theoretical and experimental time responses at 4 different frequencies that the model fits the steering compensator fairly well.

ACKNOWLEDGEMENT

We would like to thank David Cebon for making the Vehicle Dynamics Group's hydraulic ram available to us, and to John Beavis and Richard Roebuck for their assistance in the experiments.

REFERENCES

[1] S. Evangelou, D.J.N. Limebeer, R.S. Sharp and M.C. Smith, Control of Motorcycle Steering Instabilities—Passive Mechanical Compensators Incorporating Inerters, *IEEE Control Systems Magazine*, October 2006, pp. 78–88.

[2] S. Evangelou, D.J.N. Limebeer, R.S. Sharp and M.C. Smith, Mechanical steering compensation for high-performance motorcycles, *Transactions of ASME, J. of Applied Mechanics*, **74**, 332–346, 2007.

[3] L. Ljung, *System identification: Theory for the user*, Prentice Hall, 1987.

[4] B.S. Massey, *Mechanics of Fluids*, Chapman Hall, 1968.

[5] M. Nordin, J. Garlic, and P.O. Gutman, New models for backlash and gear play, *International Journal of Adaptive Control and Signal Processing*, **11**, 49-63, 1997.

[6] C. Papageorgiou, N.E. Houghton and M.C. Smith, Experimental Testing and Analysis of Inerter Devices, ASME Journal of Dynamic Systems, Measurement and Control (to appear).

[7] C. Papageorgiou, O.G. Lockwood, N.E. Houghton and M.C. Smith, Experimental testing and modelling of a passive mechanical steering compensator for high-performance motorcycles, Proceedings of the European Control Conference, Kos, Greece, July 2007, pp. 3592–3599.

[8] M.C. Smith, Force-controlling mechanical device, patent pending, International App. No. PCT/GB02/03056, priority date: 4 July 2001. http://v3.espacenet.com/textdoc?DB=EPODOC&IDX=US2005034943&F=0

[9] M.C. Smith, Synthesis of Mechanical Networks: The Inerter, *IEEE Trans. on Automat. Contr.*, **47**, 1648–1662, 2002.